Applied Energy 136 (2014) 445–453

Contents lists available at ScienceDirect

Applied Energy

journal homepage: www.elsevier.com/locate/apenergy

Strategic optimization of borehole heat exchanger field for seasonal geothermal heating and cooling

Peter Bayer [a,*], Michael de Paly [b], Markus Beck [b]

[a] ETH Zurich, Department of Earth Sciences, Sonneggstrasse 5, 8092 Zürich, Switzerland
[b] University of Tübingen, Wilhelm-Schickard-Institute for Computer Science (WSI), Sand 1, 72076 Tübingen, Germany

HIGHLIGHTS

- A procedure combining analytical simulation and linear optimization for tuning borehole heat exchanger fields is presented.
- For given heating and cooling demands the number of boreholes and their individual workloads are adjusted.
- Demonstration with a case study reveals highest optimization potential for unbalanced seasonal heating/cooling operation.

GRAPHICAL ABSTRACT

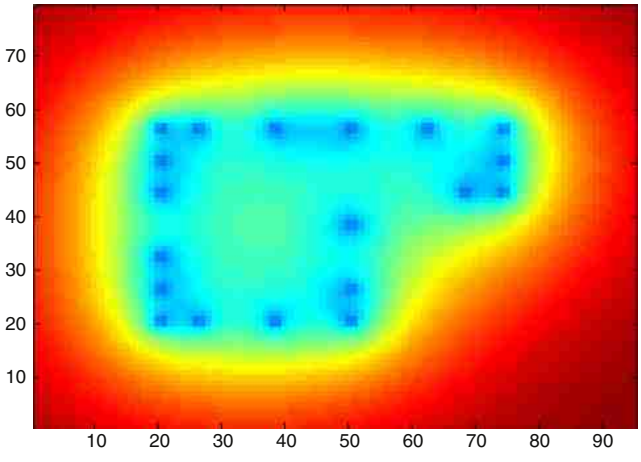

ARTICLE INFO

Article history:
Received 25 July 2014
Received in revised form 6 September 2014
Accepted 8 September 2014

Keywords:
Closed systems
Low-enthalpy geothermics
Seasonal use
Simulation
Finite line source

ABSTRACT

A mathematical procedure for optimization of borehole heat exchanger (BHE) fields is presented. If heat extraction and injection is not seasonally balanced, thermal anomalies grow in the ground. These are commonly constrained by regulations and not desirable due to potential decline of the system's performance. We demonstrate, for the case with heat extraction and only partial replenishment, how adjustment of seasonal heating and cooling workloads can mitigate local cooling of the ground. It is revealed that the benefit from mathematical optimization increases with heat extraction/injection imbalance. Evidently, strategic operation of individual BHEs in the field can to some extent compensate for the heat injection deficit. Additionally to the optimization of workloads, we inspect the required number of BHEs for a given heating/cooling demand. The idea is that by sequentially removing least effective BHEs in the field, investment cost are reduced, while the effect on the entire field performance is minimal. We show that such unfavorable BHEs exist mainly in non-optimized fields without replenishment. Thus, our work offer two ways of tuning BHE fields applied for geothermal heating and cooling: workload optimization of individual BHEs and removal of redundant BHEs for a given arrangement.

* Corresponding author. Tel.: +41 44 6336829.
E-mail address: bayer@erdw.ethz.ch (P. Bayer).

http://dx.doi.org/10.1016/j.apenergy.2014.09.029
0306-2619/

1. Introduction

The installed capacity and the utilized amount of low-enthalpy geothermal energy for heating and cooling are continuously growing worldwide [1–4]. The most popular technological variants are small scale installations, and they operate vertical boreholes, which are drilled in shallow ground (commonly <400 m, [5]). U-shaped tubes in the boreholes circulate a heat carrier fluid to exchange heat and cold with the ground, and commonly a heat pump is run to feed the heating or cooling devices of buildings. An equipped borehole is also called borehole heat exchanger (BHE), whereas the complete installation including BHE and heat pump is the ground source heat pump (GSHP). In Switzerland, for instance, we estimate that around every fourth and, in Germany, about every tenth new building is furnished with such GSHPs. Energy demand often is higher than what a single BHE can provide, and so multiple boreholes are installed and big buildings or district heating systems are supplied by operating multiple BHE fields ([6–10]).

For shallow geothermal system planning and design, a lot of experience exists meanwhile, and engineering guidelines (e.g., [11,12]) or standard planning software may be consulted to determine a length of the BHE appropriate to supply the given energy demand. Recent more sophisticated single BHE optimization studies concentrate on heat pump performance and GSHP thermodynamic optimization [13,14]. Also, a broad range of different modeling techniques are available, which can be applied to predict the effect of operating BHEs in the ground, such as the evolution of ambient ground and circulating fluid temperature (e.g., [15–24]. These models are essential means for making long-term predictions, having in mind that BHEs are often planned for decades [25]. Still, only few studies investigate the long term operational effects in the field (e.g., [26,27]). Energy extraction or injection for years, even only for seasonal use, may introduce a growing thermal anomaly in the ground. When operating multiple neighbouring BHEs in a field, the thermal reach of the individual boreholes may interfere with each other. For that reason, minimum distances are recommended between BHEs [28]. Koohi-Fayegh and Rosen [29,30] for example examined in detail the interaction between two neighbouring BHEs. It was demonstrated for exemplary cases, given a simulation period of 30 years and different borehole spacings of 4–10 m, that adjacent placement of BHEs mitigates their performance. However, thermal interaction is not found to be strong enough to decrease individual coefficient of performance by more than 10%, and this effect is controlled by the cycle of the BHEs' periodic heat input profiles. Accordingly, a distance of 7–8 m is recommended by Signorelli et al. [31] for avoiding substantial interference between BHEs. In practical applications, we find even smaller distances of around 5 m [32].

While thermal interaction among two nearby BHEs may be acceptable, interference will be more significant in arrays of multiple BHEs. Kurevija et al. [33] exposed in their modeling study how interference increases with borehole array compaction. Lazzari et al. [34] inspected BHE arrangements (spacing between 6 and 14 m) as single lines, staggered lines and square fields. It was shown for the modeled scenario that especially a compact BHE array can hardly be operated in a sustainable way, as long as heating and cooling loads during the year are not balanced. This clearly reflects the role of the governing thermal transport process in the ground in the examined scenarios. Induced thermal anomalies, and associated energy excess or deficit, are compensated by slow lateral conductive heat flow, which is least efficient for compact multiple BHE arrangement with a small outward fringe. In some cases, advective heat transport due to groundwater flow can accelerate compensation, as discussed by Zanchini et al. [35], Beck et al. [36], Hecht-Mendez et al. [37] and Ferguson [38].

Design of BHE fields is a much greater challenge than of single BHEs, but the many additional degrees of freedom also represent chances for optimization. For example, different arrangements of multiple BHEs within a given area were studied by Beck et al. [6,39]. In the latter work, we identified typical patterns of BHE positions favorable under ideal conditions with homogeneous ground and conduction only. As anticipated, mathematical BHE field position optimization suggested focusing on the area fringe in order to maximize the effect of lateral heat conduction toward the depleting BHE field. In these studies, imbalanced seasonal use was assumed and only energy extraction for heating was considered. Optimization of more balanced BHE field operation has gained attention recently in the context of hybrid systems (e.g., [40–42]). Kjellsson et al. [43], for instance, optimized combined use of solar collectors and GSHPs. They demonstrated the compensating effect of seasonally replenishing the energy deficit in the ground by feeding solar heat injection. This symbiotic combination mitigates interference between adjacent BHEs and thus facilitates closer arrangements of BHEs. Alavy et al. [44,45] point out the benefit of combining and temporally optimizing the use of conventional (e.g. cooling tower, boiler) and geothermal energy sources for supplying seasonally varying heating demands for multiple buildings. However, for the ground component, only the total borehole length was adjusted and the BHE arrangement was not in the scope.

In this paper, which builds up on our previous work, we focus on the ground devices, the BHEs. We study optimal arrangement and number for a given seasonal energy demand. For example, in de Paly et al. [46], it was shown how non-uniform loading of the BHEs can be utilized to achieve a more balanced and overall less pronounced cooling of the ground. This was demonstrated for a given hypothetical field with lattice arrangement for the conduction only case and in Hecht-Mendez et al. [37] for the case of additional horizontal groundwater flow. Beck et al. [36,39] show a similar benefit from case-specific BHE arrangement. All these studies only deal with seasonal heating, and ignore the potential of combined heating and cooling (e.g., [47–50]). This is included in the novel optimization procedure, which is developed in the following and applied to a real-case oriented BHE field with seasonally varying demands. Subsequently, first the simulation technique is introduced. It employs temporally and spatially superimposed line source equations, which are fast and traditional means for modeling the long-term temperature evolution in the ground. Then, the optimization problem is formulated and the solution procedure is presented. The purpose is alleviating the local thermal impact of BHE operation, which is often a concern in regulatory frameworks [28] or from environmental perspectives [51,52]. Finally the procedure, which involves load and BHE number adjustments, is applied to a case study.

2. Simulation and optimization procedure

2.1. Simulation

Under the assumption of an infinite homogenous underground and temperature independent soil properties the temperature change ΔT caused by a given BHE k at any relative position $(\Delta x, \Delta y)$ to the BHE and at time t can be expressed by a linear infinite line source model

$$\Delta T_{\Delta x,\Delta y}(t,q) = \frac{q}{4\pi L\lambda} Ei\left[\frac{(\Delta x^2+\Delta y^2)^{0.5}}{4\alpha t}\right] \quad (1)$$

where L is the length of the BHE, λ is the bulk thermal conductivity, α is the thermal diffusivity, and Ei the exponential integral. Parameter q is the energy transfer rate of a BHE. It is positive in case of energy extraction, that is, during heating application. It is negative in case of energy storage into the ground or during use for cooling. This model assumes that conduction is the dominant heat transport process in the ground and advection due to groundwater flow can be ignored.

In this study we consider a set of $k = 1,\ldots,n$ BHEs, which compose the BHE field. The BHEs are located at fixed positions (x_k, y_k). This allows superimposing the temperature change of all BHEs in the field to calculate the overall temperature change at any given position within the field (i,j) by taking advantage of the extensive and additive properties of energy [53–55]. This superposition yields the overall temperature change

$$\Delta T_{i,j}(t, q_{k=1,\ldots,n}) = \sum_{k=1}^{n} \Delta T_{i,j,k}(t, q_k). \tag{2}$$

In a similar way the superposition principle can be applied to temporal changes of the energy transfer rate q_k [18,54–57]. For this, the temporal change of q_k is considered as a sequence of heating/cooling pulses at $t = 1,\ldots,m$ time steps with constant load:

$$\Delta T_{i,j}(t, q_{k,l=1,\ldots,m}) = \sum_{l=1}^{m} \frac{q_l - q_{l-1}}{4\pi L\lambda} Ei\left[\frac{((i-x_k)^2 + (j-y_k)^2)^{0.5}}{4\alpha(t_m - t_l)}\right] \tag{3}$$

where $q_{k,l}$ is the load of BHE k at time step l with l running from t_{l-1} to t_l.

Because of the linearity of Eqs. (2) and (3), the spatial superposition of k BHEs and temporal superposition of varying energy transfer rates q can be combined to a single equation

$$\Delta T_{i,j}(t, q_{k,\ldots,n,1,\ldots,m}) = \sum_{l=1}^{m}\sum_{k=1}^{n} q_{k,l}\omega_{k,l}^{t,i,j} \tag{4}$$

where $\omega_{k,l}^{t,i,j}$ can be considered as the temperature impact factor of a load applied at time step l to BHE k at an arbitrary location (i,j), and it is defined by

$$\omega_{k,l}^{t,i,j} = \frac{1}{4\pi L\lambda}\left(Ei\left[\frac{((i-x)^2+(j-y)^2)^{0.5}}{4\alpha(t-t_{l-1})}\right] - Ei\left[\frac{((i-x)^2+(j-y)^2)^{0.5}}{4\alpha(t-t_l)}\right]\right). \tag{5}$$

Parameters $q_{k,l}$ and $\omega_{k,l}^{t,i,j}$ can be merged into vectors $\vec{q} = (q_{1,1},\ldots, q_{n,1},\ldots,q_{n,m})$ and $\vec{\omega}^{t,i,j} = \left(\omega_{1,1}^{t,i,j},\ldots,\omega_{n,1}^{t,i,j},\ldots,\omega_{n,m}^{t,i,j}\right)$. This yields a simplified form of Eq. (4) that has the typical form of a linear model

$$\Delta\vec{T}_{i,j}(t,\vec{q}) = \vec{q}(\vec{\omega}^{t,i,j})^T. \tag{6}$$

2.2. Optimization procedure

The optimization procedure used in this study is based on a procedure proposed by de Paly et al. [46] for heating only cases, which we extend here for mixed heating and cooling applications. The optimization procedure targets the efficiency optimization by considering the overall underground temperature changes within the BHE field. For a given energy demand, maximum efficiency is achieved if the maximum temperature change is kept to a minimum. The main motivation for this is that often regulatory constraints exist that set thresholds on maximally allowed induced temperature changes [25,28]. Moreover, extreme local cooling or heating in a field is not desirable, as this could mitigate the efficiency of the heat pump [46]. Heat conduction is a slow process and thus any thermal anomalies generated during operation of BHEs can stay for a long time. The objective function reads:

$$\text{minimize}(\max(\Delta\vec{T}_{i,j})) \tag{7}$$

By utilizing the model from Eq. (6), we get for the temperature minimization over the entire time period t

$$\arg\min(\max(\Delta\vec{T}_{i,j}(t,\vec{q}))) \quad \forall(i,j,t) \in S \tag{8}$$

In order to minimize the temperature changes within each of the single time steps l, a secondary optimization criterion is needed, which considers the maximum temperature change at each time step l:

$$\arg\min\left(\sum_{l=1}^{m}\max(\Delta\vec{T}_{i,j}(l,\vec{q}))\right) \quad \forall(i,j,t) \in S \tag{9}$$

Both optimization criteria can be combined using a weighted sum

$$\arg\min\left(w\cdot\max(\Delta\vec{T}_{i,j}(t,\vec{q})) + \sum_{l=1}^{m}\max(\Delta\vec{T}_{i,j}(l,\vec{q}))\right) \quad \forall(i,j,t) \in S \tag{10}$$

In addition to the temperature change, we also have to consider the given heating and cooling demand at each time step E_l.

In order to meet this demand, the combined extraction of storage load of all BHEs in the field must be equal to E_l.

$$E_l = \sum_{k=1}^{n} q_{k,l} \quad l = 1,\ldots,m \tag{11}$$

where E_l is positive for time steps with heating demand and negative in case of cooling.

Special care has to be taken when applying the optimization procedure to problems with mixed seasonal heating and cooling. To maximize efficiency it makes little sense to operate at the same time some BHE of the field in cooling mode and some in heating mode. While such loading patterns may be mathematically possible, they are not favorable. In order to prevent the solver to be trapped in such solutions, additional constraints for $q_{k,l}$ have to be introduced with

$$q_{k,l} > 0 \quad \forall l = 1,\ldots,m, k = 1,\ldots,n \quad E_l > 0 \tag{12}$$

in case of heating demand and

$$q_{k,l} < 0 \quad \forall l = 1,\ldots,m, k = 1,\ldots,n \quad E_l < 0 \tag{13}$$

in the cooling case.

For time periods with zero energy extraction we get

$$q_{k,l} = 0 \quad \forall l = 1,\ldots,m, k = 1,\ldots,n \quad E_l = 0 \tag{14}$$

Max-norm terms can be rewritten into the linear problem [58] by introducing an additional virtual variable z with

$$\min(z) \tag{15}$$

and the constraints

$$\begin{aligned} \Delta\vec{T}_{i,j}(l,\vec{q}) - z\vec{e} &\prec 0 \\ -\Delta\vec{T}_{i,j}(l,\vec{q}) - z\vec{e} &\prec 0 \end{aligned} \tag{16}$$

By multiple applications of this relationship and combining Eqs. (11)–(14), the problem given in Eq. (10) can be posed as the following linear optimization problem

$$\min\left(w\cdot z_0 + \sum_{l=1}^{m} z_l\right) \tag{17}$$

with the constraints

$$
\begin{aligned}
&\Delta\vec{T}_{i,j}(t,\vec{q}) - z_0 \quad \prec 0 \\
&-\Delta\vec{T}_{i,j}(t,\vec{q}) - z_0 \quad \prec 0 \quad \forall(i,j,t) \in S \\
&\Delta\vec{T}_{i,j}(l,\vec{q}) - z_l \quad \prec 0 \\
&-\Delta\vec{T}_{i,j}(l,\vec{q}) - z_l \quad \prec 0 \quad \forall(i,j,l) \in S \quad l = 1,\ldots,m \\
&E_l = \sum_{k=1}^{n} q_{k,l} \qquad l = 1 \ldots m \\
&q_{k,l} > 0 \qquad E_l > 0 \\
&q_{k,l} < 0 \qquad E_l < 0 \\
&q_{k,l} = 0 \qquad E_l = 0
\end{aligned}
\tag{18}
$$

This problem can now be solved by any linear optimization technique that is capable of dealing with the resulting large number of optimization variables $q_{k,l}$ and constraints.

2.3. BHE number reduction

When operating a BHE field over years, interference among the individual boreholes will increase as a consequence of growing energy deficit and due to generally slow natural heat conduction that can compensate it [12,27]. During the course of a BHE field lifetime, this yields to more pronounced differences in the performance of individual BHEs in the field. Especially in the center of the field, competition for conductive heat supply in the ground is highest, and as a consequence, most beneficial are those BHEs at the fringe of a BHE. This is examined for example in Beck et al. [39], where equal loads and equal heat carrier flows both lead to strongest ground cooling in the center of a quadratic field utilized for heating only (see also [34]). It is demonstrated that when individual BHE positions are optimized, they are arranged in typical geometries with strong focus at the margin of a feasible area. Apparently this maximizes the compensating effect of lateral heat conduction.

As an alternative to BHEs that are "moving" during a computationally demanding optimization procedure, we here investigate the potential of iterative BHE reduction. The suggested strategy is (i) start with all BHEs and optimize workloads according to Eq. (17) for supplying the given heat and cold demand; (ii) this field is run with equal workloads at the BHEs; (ii) the most-critical BHEs are identified, where maximum decline of the ground temperature is measured; (iii) a given number (one or more) of most-critical BHEs is removed; (iv) workload optimization is repeated for the BHE field of reduced size; continued by step (ii) until a minimum number of BHEs is reached. Note that equally distributed loads are chosen for finding critical BHE positions rather than optimized loads, because optimization would minimize local cooling and interference between neighbouring BHEs. Thus, here individual BHE load optimization (Eq. (17)) is used to tune the BHE field of reduced size and, this way, examine the best performance feasible after potentially redundant BHEs are removed.

The suggested iterative procedure will reveal if it is possible to operate a BHE field with less BHEs (to save borehole meters, material) without taking substantial losses in efficiency. A premise is that while reducing the number of boreholes of an already planned field, always the same seasonal energy demand has to be fulfilled (for heating and cooling). In the following application case, consequences from iterative BHE reduction to the ground temperature and heat carrier fluid temperature in the BHEs are analyzed.

3. Study case

Our application case is oriented at a real site close to Nuremberg in Franconia, Germany. The borehole field consists of 54 BHEs, each with 78 m depth, which are installed within a 36 m × 54 m area (Fig. 1). The distance between adjacent BHEs, all arranged in a lattice, is regularly 6 m. This value is on the lower end of recommended distances, and thus thermal interference between neighbouring BHEs can be expected to occur already early within the time of operation. We limit our study on the first 15 years of operation, although at the real site, a longer time horizon is assumed. The time-dependent energy profile represents the energy extraction, respectively injection rates, which are needed to supply the demand of a new building at the site. By strategic distribution as time-dependent BHE workloads the field is ultimately optimized. In our demonstration case, the originally monthly energy demand profile is upscaled and approximated by a coarser quarterly profile (Fig. 2). This is done by summarizing three consecutive time steps of one month length to one large time step of three months length. This yields four time steps per year, which represent a heating period (Dec.–Feb.), a cooling period (Jun.–Aug.) and two transition periods (Mar.–May, Sep.–Nov.). By the proposed simplifications in operation time and temporal resolution, the computational burden is kept at reasonable level, while focus is set on the optimization procedure.

The ground is approximated as homogeneous, isotropic media, with constant temperature at initial stage. Groundwater flow is negligible and thus heat in the ground is only transported by conduction. Parameter values describing the conditions at the site are listed in Table 1. These are used for simulation with the spatially and temporally superimposed finite line source equations.

The BHE field's total annual heat extraction accrues to 239.24 MW h, whereas heat injection is considered a variable. In the following, however, in different scenarios these values are varied in order to examine the sensitivity of (optimized) BHE performance to the relative amount of heating and cooling. In another scenario, we envisage the possibility of reducing the predefined total number of BHEs while delivering the given heat and cold demand.

4. Results

4.1. Effect of cooling ratio

This section presents a sensitivity analysis to determine (i) the maximum temperature changes in the ground, $\max(\Delta T_{i,j})$, and (ii) the possible improvement by individual BHEs' workload optimization. Both aspects are inspected for variable amounts of injected cooling energy during summer months. For this purpose, the

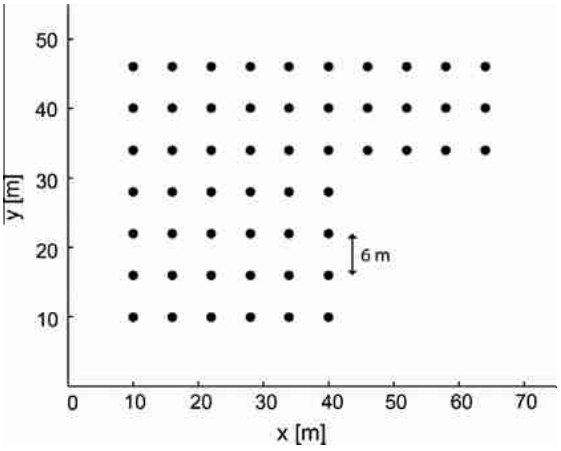

Fig. 1. Lattice arrangement of BHEs from case study; grid distance is 6 m and total number of BHEs is 54. Origin of coordinate system is arbitrary.

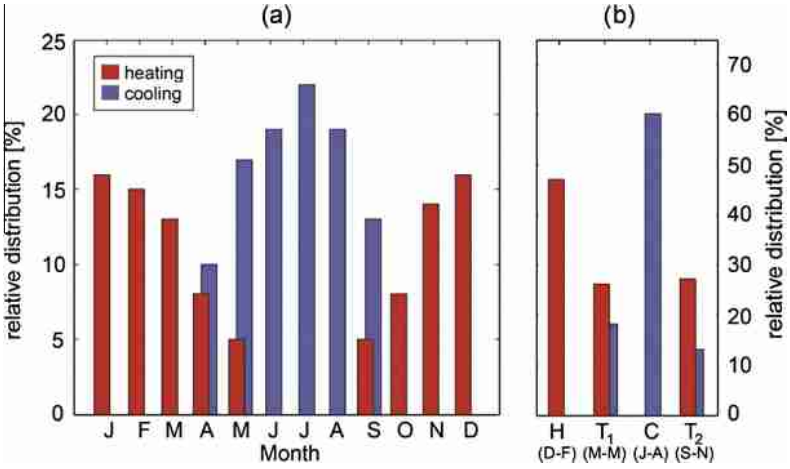

Fig. 2. (a) Original monthly heating and cooling demand for case study, and (b) upscaled quarterly schedule with heating (H), cooling (C) and two transition periods (T_1, T_2).

Table 1
Parameter specifications for case study.

Parameter	Value
Porosity, n	0.46
Ground thermal conductivity, λ	2.8 W m^{-1} K^{-1}
Ground thermal diffusivity, α	8.24×10^{-7} m^2 s^{-1}
Ground volumetric heat capacity, c_p	3.4×10^6 J m^{-3} K^{-1}
Borehole length, h	78 m

annual extracted heat demand of the BHE field is kept constant at the case-specific value of 239.24 MW h, while the injected annual cooling energy is increased stepwise by 5% of the extracted annual heat energy, i.e. 0 MW h (only heating mode), 11.96 MW h, 23.92 MW h, etc. The temperature changes in the ground, $\Delta T_{i,j}$, are determined in 39 m depth, which corresponds to the half of the installed depth of the BHEs. The values of $\max(\Delta T_{i,j})$ are measured in 0.5 m distance to the BHE positions (see e.g. [46]). By optimization as formulated in Eq. (17), this maximum temperature change in the ground is minimized and balanced energy extraction/injection strategies are identified.

Since the temperature change in the ground is linearly dependent on the given BHE workload (see Eq. (4)) and cooling can also be expressed as heating with a negative sign, the function which describes the relationship between injected cooling energy and $\max(\Delta T_{i,j})$ is expected to be also linear. This is confirmed by the calculated maximum ground temperatures for variable cooling rates depicted in Fig. 3. These represent the conditions after the heating phase of the penultimate time step for optimized and non-optimized (equal) workloads. Note that no higher cooling ratios than 90% were inspected, because differences between optimized and non-optimized variants become so low for cooling ratios close to 100% reaching a range biased by model inaccuracies. Apparently full seasonal replenishment of the ground makes workload optimization redundant and represents the ideal case for sustainable operation. In contrast, the benefit from optimization rises when reducing the cooling ratio.

For the examined case study, without optimization, ground temperatures reach small values that are nearly $\max(\Delta T_{i,j}) = 15$ K below the original value. With ambient ground temperatures of around 11 °C at the site this would mean local freezing. This is visualized in the temperature maps for the BHE field in 39 m depth (Fig. 4c). Choosing equal loads for all BHEs cools out the ground and freezing would occur in the central part of the field. This demonstrates the need for partial seasonal energy replenishment. Fig. 4d reveals much less pronounced ground cooling when 50%

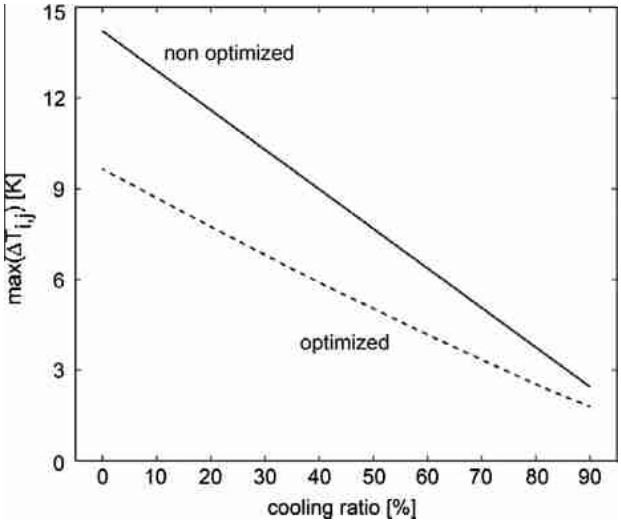

Fig. 3. Comparison between non-optimized and optimized BHE fields: depending on the replenishment of the induced energy deficit in the ground (cooling ratio), the degree of local ground cooling, $\max(\Delta T_{i,j})$, can be mitigated.

of the extracted energy is replenished during the summer season. However, more balanced use of the ground is also feasible by operating optimized workloads, with a maximum temperature decline of only around 10 K for the heating-only variant. Such decline can be reached without workload optimization only by a cooling ratio of at least 35% (Fig. 3). As depicted in Fig. 4a, optimization yields a smoothed spatial temperature distribution without extremes and less significant thermal gradients. Overall, for cooling ratios from 0% to 80%, the improvement (in $\max(\Delta T_{i,j})$) achieved by optimization ranges between 32% and 34%. For higher cooling ratios the improvement declines slightly to 27%. This reduced benefit from optimization is illustrated by the thermal BHE field maps, comparing the improvement without cooling (Fig. 4a and c) and with 50% cooling (Fig. 4b and d).

In practice, contrasting the linear trends in Fig. 3 based on a few heating–cooling variants can easily be used to judge the potential of workload optimization. For a given regulatory restriction on maximum induced temperature variation in the ground, the minimum required cooling energy for equally distributed and optimized options can be estimated. This delivers the required energy to be injected into the ground during summer months to keep the ground temperature changes within the allowed ranges.

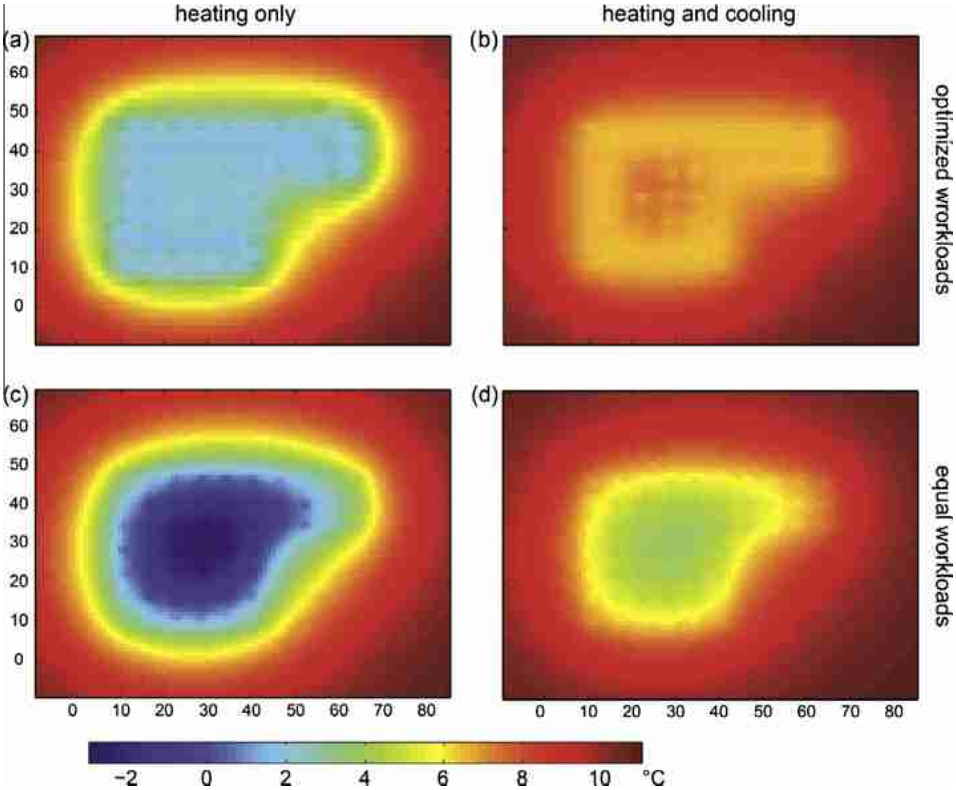

Fig. 4. Thermal conditions in ground at half of the BHE depth (39 m) after 15 years of operation for (a and c) heating only, and (b and d) heating and 50% cooling. Thermal anomalies are more pronounced for (c and d) non-optimized, equal workloads than (a and b) when individually optimized for the BHEs.

Additionally, alternative technological variants such as the BHE field operated with equal heat carrier flow rates [46] can visually be compared. Furthermore, uncertainty bounds may be added that account for predictive uncertainties (e.g. due to variation in expected energy demand profiles), and modeling inaccuracies (e.g., in geological parameters).

4.2. Optimization of heating/cooling scenarios with reduced number of BHEs

Increasing the cooling ratio will promote regeneration of the BHE field. Alternatively, when a more balanced and sustainable operation can be achieved, then theoretically less BHEs could be needed for supplying the energy demand. This is studied in this chapter by applying an iterative BHE number reduction to conditions with different heating ratios.

The case study (Fig. 1) with given lattice arrangement of 54 BHEs is selected as reference. We decided for a maximum mean workload of 50 W/m for each single BHE as termination criterion. This corresponds, in case of equally distributed workloads, to a BHE field of at least 20 instead of 54 BHEs. So a total number of 34 reductive iterations are applied. Operation time remains unchanged, and results are inspected for the conditions after 15 years. Main questions are, how will the temperature in the BHE field be influenced, and will there be more local cooling? We also ask what will be the effects on the fluid temperature in the pipes.

Fig. 5 shows the development of the maximum temperature change in the ground dependent on the number of BHEs for optimized and equally distributed workloads and four different cooling ratios (0%, 25%, 50%, and 75%). The simulations were accomplished with the finite line source model and temperatures were calculated again in 39 m depth. Fig. 6 depicts BHE positions after 0 (a), 4 (b), 14 (c), 24 (d) and 34 (e) iterations of the BHE reduction algorithm. As expected, for the simulations with non-optimized workloads, $\max(\Delta T_{i,j})$ first starts to decrease significantly, because the BHE field thins out at the positions with strongest BHE interactions (Fig. 6). As expected, the chosen potentially redundant positions are found in the center of the original field and during the course of the procedure the given field hollows out. During the first iterations the relative increase of the loads is much smaller than at later

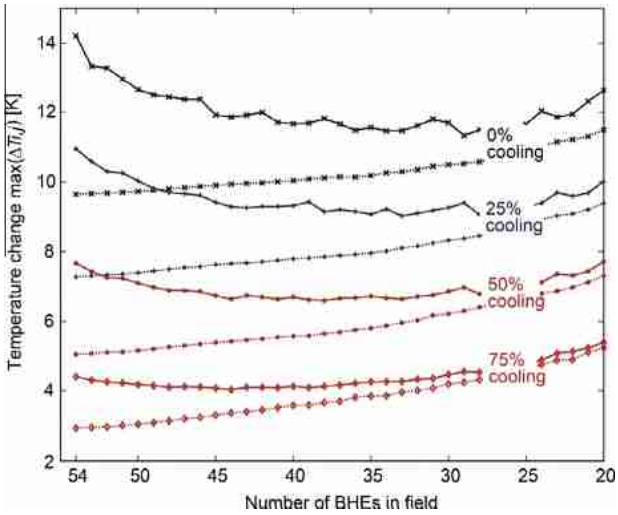

Fig. 5. Effect of BHE reduction on induced maximum ground thermal anomalies for optimized (dotted) and non-optimized (continuous) variants. For the four different cooling cases (no cooling, 25%, 50%, 75% replenishment), selective removal of BHEs can help moderating local anomalies for non-optimized systems operated at equal workloads.

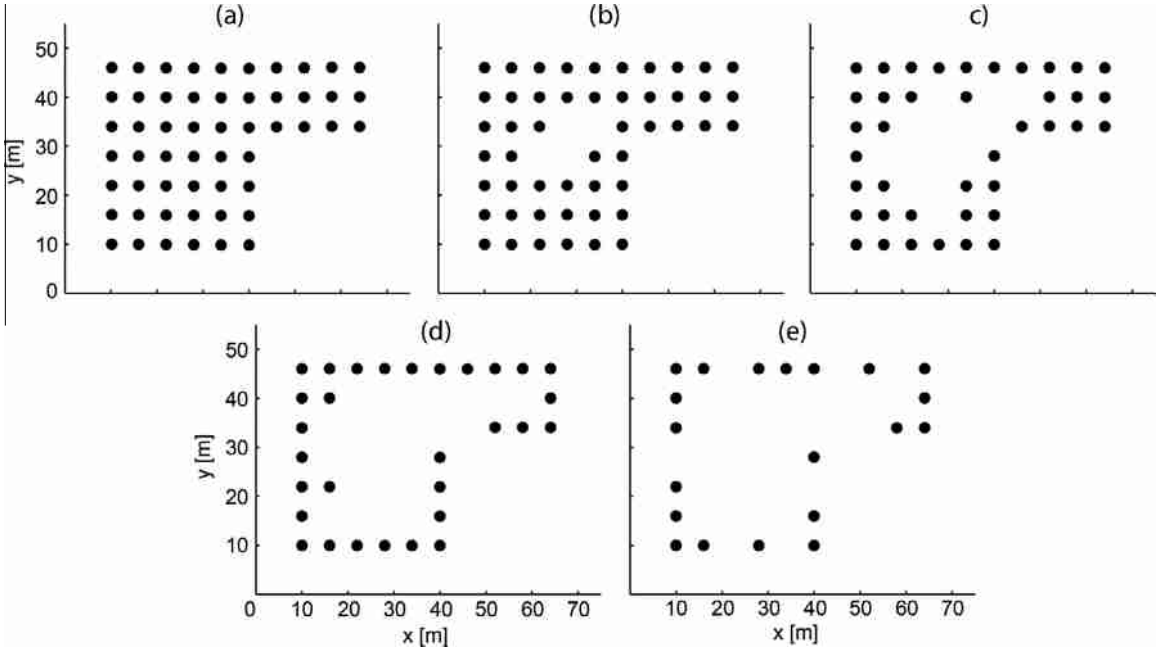

Fig. 6. Illustration of BHE field evolution during selective removal of individual BHEs, starting with (a) 54 BHEs in lattice arrangement, leading to central thinning of the field with (b) 50, (c) 40, (d) 30, and (e) 20 residual BHEs.

iterations. For example, reducing the number of BHEs from 54 to 53 means an on the average 1.8% higher workload for each BHE. When reducing it from 25 to 24 BHEs, individual loads increase on the average by 4%. For this reason, the $\max(\Delta T_{i,j})$ curve (Fig. 5) initially decreases for all four cooling rates until a reversal point is reached. From this point, the $\max(\Delta T_{i,j})$ curve starts to ascend, and increasing BHE loads exceed the benefits gained by the removal of most critical BHEs. By operating less BHEs local cooling accelerates.

For higher cooling rates, the $\max(\Delta T_{i,j})$ drop is less pronounced at the beginning, and the reversal point moves more to the left, that is, there is a smaller benefit from removing BHEs (Fig. 5). This reflects that BHE fields operated in a mixed heating/cooling mode have a higher capacity to regenerate or to compensate negative effects due to BHE interaction than fields, which are operated exclusively in heating mode. In comparison, the $\max(\Delta T_{i,j})$ curves for optimized BHE workloads exhibit lower values and are monotonically increasing throughout all iterations. This indicates that negative effects on ground temperature due to BHE interactions can well be compensated by workload optimization.

An important criterion for the performance of a GSHP is the fluid temperature in the BHE pipes. Further, there exist directives, which set a tolerance threshold for induced temperature difference between heat-carrier fluid and undisturbed ground during continuous operation, and which in many cases serve as basis for the approval of GSHP systems. We therefore inspect the temporal evolution for the average temperature at the borehole wall, which is considered a proxy for the heat carrier fluid temperature, which will ultimately determine the performance of the heat pump. It is derived by estimating the average temperature on a circle of 0.5 m around the BHE position.

Fig. 7 shows the effect of seasonally variable energy extraction and injection, resulting in undulating trends of the average borehole temperatures. Since extracted energy is not fully replenished, these trends are all declining on the long-term. Heat conduction in the ground is not sufficient to compensate the induced deficits. For

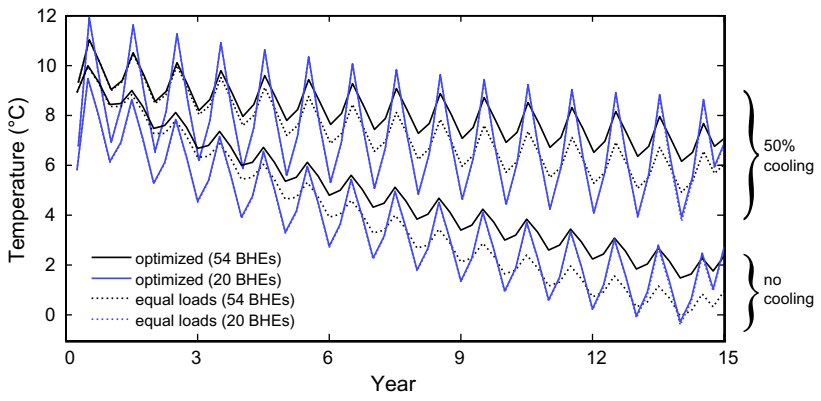

Fig. 7. Evolution of simulated mean borehole wall temperature in the field during operation for 15 years. Undulating curves are derived due to seasonal operation, for scenarios with optimized and equal workloads, no cooling and 50% replenishment, the full set of 54 and the minimum number of 20 BHEs.

the case with 50% cooling, the seasonal amplitudes are more pronounced, which is apparently due to the enhanced recovery by cooling during the summer period. The figure shows for both cases, with and without cooling, that the use of all 54 BHEs benefits from optimization. Calculated borehole temperatures tend to decline more without optimization and after 15 years of operation reach values, which are by 1–2 K lower. Additionally are shown the scenarios with a minimum number of 20 BHEs, with and without cooling. As expected, the temperatures are generally lower and more seasonally variable in comparison to the results for the full BHE field. It is also demonstrated that after systematic thinning out of the BHE field, additional optimization of BHE operation mode can hardly improve the temperature. This is valid with and without cooling (see also Fig. 5). These findings for combined workload optimization and BHE number reduction can be compared with those by Beck et al. [39], where it is shown that combined adjustment of BHE workloads and positions offers only minor benefits in comparison to either workloads or positions as decision variables.

5. Conclusions

The presented work expands on previously developed mathematical optimization techniques for the ground devices of shallow geothermal energy application. The objective is to ideally adjust vertical borehole heat exchangers (BHEs) in large BHE fields. Our main contribution here is the combined optimization of individual BHE workloads for seasonal heating and cooling. A linear optimization problem is formulated that can be efficiently solved by standard linear programming techniques. It is shown for the selected case study that the thermal impact on the long-term conditions in the ground can be minimized while supplying a given heating and cooling demand. Induced thermal anomalies are less extreme and smoothened by optimization. As a consequence, average borehole temperatures are raised, and this affects the performance of the entire GSHP system. Alternatively, this optimization procedure could also be employed for maximizing the energy exchange with the ground, given regulative constraints that commonly are in force for limiting ground heating or cooling.

Standard arrangements of BHEs are oriented at regular grids. As shown previously, including the position of BHEs implicitly in the optimization problem can similarly be utilized for system tuning as individual borehole adjustment [39]. Both strategies will enforce uniform heat exchange with the ground. As a third option we here examine the effect of reducing the number of boreholes, starting with those that stimulate strongest thermal impacts. It is shown for the reference case, for which equal workloads among all BHEs are assumed, that it is desirable removing the BHEs located centrally in the field. At these positions, lateral conductive heat supply in the ground is prohibited by the existence of surrounding BHEs. As a result, this sequential procedure yields arrangements with BHEs concentrated along the fringe of the original field. This is similar to the findings from BHE position optimization, which moves BHEs away from the center. Technically, sequential BHE reduction until a certain limit (on individual BHE workload, ground thermal impact, etc.) is reached appears an attractive alternative to implicit position optimization. Resulting arrangements are still along a grid, and fast linear programming can be applied rather than computationally demanding global optimization techniques such as evolutionary algorithms, which are necessary for moving BHEs.

Acknowledgements

This work was supported by the Deutsche Bundesstiftung Umwelt (DBU) and, within the Geotherm-II project, by the Competence Center Energy and Mobility and Competence Center for Environment and Sustainability of the ETH-Domain. We thank Gabi Moser for language corrections and Waldemar Retkovski for fruitful discussions.

References

[1] Bayer P, Saner D, Bolay S, Rybach L, Blum P. Greenhouse gas emission savings of ground source heat pump systems in Europe: a review. Renew Sust Energ Rev 2012;16:1256.
[2] Self SJ, Reddy BV, Rosen MA. Geothermal heat pump systems: status review and comparison with other heating options. Appl Energ 2013;101:341.
[3] Spitler JD. Ground-source heat pump system research – past, present, and future. Hvac&R Res 2005;11:165.
[4] Florides GA, Christodoulides P, Pouloupatis P. An analysis of heat flow through a borehole heat exchanger validated model. Appl Energ 2012;92:523.
[5] Hecht-Mendez J, Molina-Giraldo N, Blum P, Bayer P. Evaluating MT3DMS for heat transport simulation of closed geothermal systems. Ground Water 2010;48:741.
[6] Beck M, Hecht-Mendez J, de Paly M, Bayer P, Blum P, Zell A. Optimization of the energy extraction of a shallow geothermal system. IEEE C Evol Computat 2010.
[7] Dagdas A. Heat exchanger optimization for geothermal district heating systems: a fuel saving approach. Renew Energ 2007;32:1020.
[8] Desideri U, Sorbi N, Arcioni L, Leonardi D. Feasibility study and numerical simulation of a ground source heat pump plant, applied to a residential building. Appl Therm Eng 2011;31:3500.
[9] Herbert A, Arthur S, Chillingworth G. Thermal modelling of large scale exploitation of ground source energy in urban aquifers as a resource management tool. Appl Energ 2013;109:94.
[10] Sanner B, Mands E, Sauer MK. Larger geothermal heat pump plants in the central region of Germany. Geothermics 2003;32:589.
[11] Kavanaugh SP, Rafferty KD. Ground-source heat pumps: design of geothermal systems for commercial and institutional buildings. American Society of Heating, Refrigerating and Air-Conditioning Engineers; 1997.
[12] Stauffer F, Bayer P, Blum P, Molina-Giraldo N, Kinzelbach W. Thermal use of shallow groundwater. CRC Press; 2013.
[13] Li M, Lai ACK. Thermodynamic optimization of ground heat exchangers with single U-tube by entropy generation minimization method. Energ Convers Manage 2013;65:133.
[14] Sivasakthivel T, Murugesan K, Thomas HR. Optimization of operating parameters of ground source heat pump system for space heating and cooling by Taguchi method and utility concept. Appl Energ 2014;116:76.
[15] Carslaw H, Jaeger J. Heat in solids. Oxford: Clarendon Press; 1959.
[16] Casasso A, Sethi R. Efficiency of closed loop geothermal heat pumps: a sensitivity analysis. Renew Energ 2014;62:737.
[17] Li SH, Yang WH, Zhang XS. Soil temperature distribution around a U-tube heat exchanger in a multi-function ground source heat pump system. Appl Therm Eng 2009;29:3679.
[18] Marcotte D, Pasquier P. Fast fluid and ground temperature computation for geothermal ground-loop heat exchanger systems. Geothermics 2008;37:651.
[19] Molina-Giraldo N, Bayer P, Blum P. Evaluating the influence of thermal dispersion on temperature plumes from geothermal systems using analytical solutions. Int J Therm Sci 2011;50:1223.
[20] Rees SJ, He MM. A three-dimensional numerical model of borehole heat exchanger heat transfer and fluid flow. Geothermics 2013;46:1.
[21] Wagner V, Bayer P, Kubert M, Blum P. Numerical sensitivity study of thermal response tests. Renew Energ 2012;41:245.
[22] Zarrella A, Capozza A, De Carli M. Analysis of short helical and double U-tube borehole heat exchangers: a simulation-based comparison. Appl Energ 2013;112:358.
[23] Li M, Lai AC. Analytical model for short-time responses of ground heat exchangers with U-shaped tubes: model development and validation. Appl Energ 2013;104:510.
[24] Bouhacina B, Saim R, Benzenine H, Oztop HF. Analysis of thermal and dynamic comportment of a geothermal vertical U-tube heat exchanger. Energ Build 2013;58:37.
[25] Hahnlein S, Bayer P, Ferguson G, Blum P. Sustainability and policy for the thermal use of shallow geothermal energy. Energ Policy 2013;59:914.
[26] Kim SK, Bae GO, Lee KK, Song Y. Field-scale evaluation of the design of borehole heat exchangers for the use of shallow geothermal energy. Energy 2010;35:491.
[27] Rybach L, Eugster WJ. Sustainability aspects of geothermal heat pump operation, with experience from Switzerland. Geothermics 2010;39:365.
[28] Haehnlein S, Bayer P, Blum P. International legal status of the use of shallow geothermal energy. Renew Sust Energ Rev 2010;14:2611.
[29] Koohi-Fayegh S, Rosen MA. Examination of thermal interaction of multiple vertical ground heat exchangers. Appl Energ 2012;97:962.
[30] Koohi-Fayegh S, Rosen MA. An analytical approach to evaluating the effect of thermal interaction of geothermal heat exchangers on ground heat pump efficiency. Energ Convers Manage 2014;78:184.
[31] Signorelli S, Kohl T, Rybach L. Sustainability of production from borehole heat exchanger fields. In: 29th Workshop on geothermal reservoir engineering; 2004. p. 1.

[32] Fossa M, Minchio F. The effect of borefield geometry and ground thermal load profile on hourly thermal response of geothermal heat pump systems. Energy 2013;51:323.
[33] Kurevija T, Vulin D, Krapec V. Effect of borehole array geometry and thermal interferences on geothermal heat pump system. Energ Convers Manage 2012;60:134.
[34] Lazzari S, Priarone A, Zanchini E. Long-term performance of BHE (borehole heat exchanger) fields with negligible groundwater movement. Energy 2010;35:4966.
[35] Zanchini E, Lazzari S, Priarone A. Long-term performance of large borehole heat exchanger fields with unbalanced seasonal loads and groundwater flow. Energy 2012;38:66.
[36] Beck M, de Paly M, Hecht-Mendez J, Bayer P, Zell A. Evaluation of the performance of evolutionary algorithms for optimization of low-enthalpy geothermal heating plants. In: Proceedings of the fourteenth international conference on genetic and evolutionary computation conference; 2012. p. 1047.
[37] Hecht-Mendez J, de Paly M, Beck M, Bayer P. Optimization of energy extraction for vertical closed-loop geothermal systems considering groundwater flow. Energ Convers Manage 2013;66:1.
[38] Ferguson G. Screening for heat transport by groundwater in closed geothermal systems. Groundwater 2014.
[39] Beck M, Bayer P, de Paly M, Hecht-Mendez J, Zell A. Geometric arrangement and operation mode adjustment in low-enthalpy geothermal borehole fields for heating. Energy 2013;49:434.
[40] Hackel S, Pertzborn A. Effective design and operation of hybrid ground-source heat pumps: three case studies. Energ Build 2011;43:3497.
[41] Park H, Lee JS, Kim W, Kim Y. Performance optimization of a hybrid ground source heat pump with the parallel configuration of a ground heat exchanger and a supplemental heat rejecter in the cooling mode. Int J Refrig 2012;35:1537.
[42] Park H, Lee JS, Kim W, Kim Y. The cooling seasonal performance factor of a hybrid ground-source heat pump with parallel and serial configurations. Appl Energ 2013;102:877.
[43] Kjellsson E, Hellstrom G, Perers B. Optimization of systems with the combination of ground-source heat pump and solar collectors in dwellings. Energy 2010;35:2667.
[44] Alavy M, Dworkin SB, Leong WH. A design methodology and analysis of combining multiple buildings onto a single district hybrid ground source heat pump system. Renew Energ 2014;66:515.
[45] Alavy M, Nguyen HV, Leong WH, Dworkin SB. A methodology and computerized approach for optimizing hybrid ground source heat pump system design. Renew Energ 2013;57:404.
[46] de Paly M, Hecht-Mendez J, Beck M, Blum P, Zell A, Bayer P. Optimization of energy extraction for closed shallow geothermal systems using linear programming. Geothermics 2012;43:57.
[47] Liu Y, Qin XS, Chiew YM. Investigation on potential applicability of subsurface cooling in Singapore. Appl Energ 2013;103:197.
[48] Pahud D, Belliardi M, Caputo P. Geocooling potential of borehole heat exchangers' systems applied to low energy office buildings. Renew Energ 2012;45:197.
[49] Sagia Z, Rakopoulos C, Kakaras E. Cooling dominated hybrid ground source heat pump system application. Appl Energ 2012;94:41.
[50] Younger JS, Booth DJ, Kurniawan K. Sustainable development – the East Bali poverty project. P I Civil Eng-Munic 2012;165:43.
[51] Brielmann H, Lueders T, Schreglmann K, Ferraro F, Avramov M, Hammerl V, et al. Shallow geothermal energy usage and its potential impacts on groundwater ecosystems. Grundwasser 2011;16:77.
[52] Ferguson G. Subsurface energy footprints. Environ Res Lett 2013:8.
[53] Diao N, Li Q, Fang Z. Heat transfer in ground heat exchangers with groundwater advection. Int J Therm Sci 2004;43:1203.
[54] Michopoulos A, Kyriakis N. A new energy analysis tool for ground source heat pump systems. Energy Build 2009;41:937.
[55] Marcotte D, Pasquier P, Sheriff F, Bernier M. The importance of axial effects for borehole design of geothermal heat-pump systems. Renew Energ 2010;35:763.
[56] Eskilson P. Thermal analysis of heat extraction boreholes. University of Lund, Lund: Department of Mathematical Physics; 1987.
[57] Bernier MA, Pinel P, Labib R, Paillot R. A multiple load aggregation algorithm for annual hourly simulations of GCHP systems. HVAC & R Res 2004;10:471.
[58] Boyd S, Vandenberghe L. Convex optimization. Cambridge: Cambridge University Press; 2004.